

Friction Control in Thin-Film Lubrication

Jianping Gao, W. D. Luedtke, and Uzi Landman*

School of Physics, Georgia Institute of Technology, Atlanta, Georgia 30332-0430

Received: May 6, 1998

A novel method is proposed for controlling and reducing friction in thin-film boundary lubricated junctions, through coupling of small amplitude (of the order of 1 Å) directional mechanical oscillations of the confining boundaries to the molecular degrees of freedom of the sheared interfacial lubricating fluid. Extensive grand-canonical molecular dynamics simulations revealed the nature of dynamical states of confined sheared molecular films, their structural characteristics, and the molecular scale mechanisms underlying transitions between them. Control of friction in the lubricated junction is demonstrated, with a transition from a high-friction stick–slip shear dynamics of the lubricant to an ultralow kinetic friction state (termed as a superkinetic friction regime), occurring for Deborah number values $D_e = \tau_f/\tau_{osc} > 1$, where τ_{osc} is the time constant of the boundary mechanical oscillations normal to the shear plane and τ_f is the characteristic relaxation time for molecular flow and ordering processes in the confined region. A rate and state model generalized to include the effects of such oscillations is introduced, yielding results in close correspondence with the predictions of the atomistic simulations.

Understanding the atomic-scale origins of the mechanical and rheological properties of boundary lubricating thin molecular films, confined between closely spaced solid boundaries, is of fundamental and technological interest, aiming at molecular design of lubricants for use under extreme conditions of high loads and shear rates.^{1–3} Confined fluids have been observed experimentally and theoretically to exhibit unique structural, dynamical, mechanical, and rheological properties, different from those of the bulk and dependent on the degree of confinement (load), operational conditions (e.g., shear rate and temperature), and nature of the fluid (e.g., molecular shape, size, and complexity) and its interactions with the boundaries (e.g., chemical or physical binding).^{1–12} These properties include organization of interfacial films into layered structures characterized by load-sustaining capacity portrayed in oscillatory solvation forces between the confining surfaces as the gap width between them is varied, and confinement-induced dynamical rheological response characteristics such as long-relaxation times, the development of shear yield stresses (static friction), and the occurrence of classes of shear motion (e.g., stick–slip and a transition to a steady sliding state and to an eventual state of ultralow kinetic friction (termed the superkinetic regime¹³) for shear velocities exceeding a critical value, v_c).

Here we investigate, through molecular dynamics (MD) simulations, novel mechanisms for modifying, controlling, and reducing frictional resistance in thin-film boundary lubrication, through dynamical directional coupling to the sheared fluid of small-amplitude mechanical oscillatory motion of the confining surfaces, applied normal to the shear plane.

Underlying the aforementioned properties of confined molecular films and their tribological response are microscopic momentum and energy transfer mechanisms governed by couplings between the lubricating film molecules and the (mechanical) motion of the shearing boundaries, as well as between intra- and intermolecular degrees of freedom. Associated with such couplings is a spectrum of characteristic times (τ_f) (materials, temperature, and load dependent) for dynamic

structural (and conformational) relaxations and energy redistribution and dissipation, as well as system characteristic times (operationally dependent) such as the mechanical drive time $\tau_{drive} = \lambda/v$, which is the time for driving the systems at a velocity v a characteristic distance λ . The ratio $D_e = \tau_f/\tau_{drive}$ is defined as the Deborah number,¹⁴ and it is expected that different regimes of rheological response correspond to different values of D_e , which may be accessed for a given lubricant (as well as given temperature and load) through control of τ_{drive} . Thus, it is expected that dissipation will be maximal for $D_e \sim 1$, and otherwise reduced friction will occur.¹⁵

The MD simulations were performed using our recently developed grand-canonical MD (GCMD) method.¹² In this method, which models the configuration used in the surface force apparatus (SFA)^{1,4} and tip-based^{1,3} experiments, the periodically replicated simulation cell contains two opposing solid blocks with a gap D between them (along the z -direction normal to the solid surfaces) immersed in a liquid, such that the liquid in the confined region is at dynamic equilibrium with the surrounding liquid. The solid blocks are of finite size in the x -direction and extend over the length of the simulation cell in the y -direction. The size of the cell in the x -direction, H_x , is taken to be sufficiently large so that the molecules outside the confinement can exhibit bulk liquid behavior and the length H_x varies dynamically using constant pressure MD (with $P_{ext}^x = 1$ atm). The geometrical parameters used in the simulations are given in ref 12b.

In the simulations of shear the direction of sliding is along the y -axis. In these simulations the upper solid block is connected to a horizontal (y) spring (spring constant $k_s = 0.8$ N/m), which is pulled at a constant velocity v_s . To model constant load conditions, the center of mass of the block in the z -direction, z_{cm} , varies dynamically in response to the balance between an externally applied load, P_{ext}^z and the z -component of the internal stress exerted by the liquid molecules on the upper block, σ_{int}^{zz} , i.e., $(M/A)\ddot{z}_{cm} = P_{ext}^z - \sigma_{int}^{zz}(t)$, where M is the mass of the block and A is its area. In addition, simulations

were performed where the gap width was modulated periodically in time using a triangular drive (modeling a time-varying externally applied load).

The fluid (spherical) molecules were treated dynamically using 6–12 Lennard-Jones (LJ) interactions, with ϵ and σ parameters as described in ref 12b, corresponding to a commensurate solid–liquid system;¹⁶ i.e., fcc solid blocks¹⁷ with a lattice constant $a = 5.798 \text{ \AA}$, exposing (111) surfaces, were used in conjunction with a liquid whose LJ parameters were taken as $\epsilon/k_B = 119.8 \text{ K}$ and $\sigma = 3.405 \text{ \AA}$, corresponding to the solid and bulk liquid having the same density at the temperature of the simulations, $k_B T = 0.835\epsilon$ (above the melting temperature of the bulk LJ material at $P = 1 \text{ atm}$).

For gap widths $D \leq 30 \text{ \AA}$, the confined liquid organizes into layered structures normal to the boundaries.^{12b} The degree of ordering into such layers depends on D , and it originates^{12b} from variations in the internal energy and entropic contributions to the free energy which oscillates (as well as the corresponding solvation forces) as a function of D . Well-formed layers (i.e., states of maximum sharpness of the oscillations of the density profiles, $\rho(z)$, across the film, which are characterized by minima of the in-layer diffusion^{12b}), occur with a period of about the molecular width ($\sim 4 \text{ \AA}$). As elaborated by us previously,^{12b} transitions between such well-formed equilibrium layered states (occurring here for $D_{n_L} = 26, 22, 18, 15, 12$, and 9 \AA , corresponding to $n_L = 7, 6, 5, 4, 3$, and 2 layers, see Figures 1 and 2 in ref 12b), are associated with expulsion of about a layer-worth of molecules from the confined region. Most important here is the observation¹² that such molecular expulsion transitions occur (for globular molecules and straight-chain alkanes) discontinuously (reflected in a steplike drop pattern in the number of confined molecules, n_c , as a function of D), and they are caused by a relatively small reduction of the gap width ($\delta \sim 1 \text{ \AA}$). Further reduction of the gap width in the interval $D_{n_L} - D_{n_L-1} - \delta$ occurs for an almost constant number of molecules in the confinement and is accompanied by enhancement of the interlayer (and intralayer) order in the resulting $(n_L - 1)$ -layered film.

Results of constant load ($P_{\text{ext}}^z = 73 \text{ MPa}$) shear simulations of an equilibrated four-layer liquid film (with ~ 150 molecules per layer) for three spring-pulling velocities v_s are shown in Figure 1. A characteristic stick–slip sliding motion is found for the lower velocity (1 m/s), approaching a steady sliding state for $v_s = 20 \text{ m/s}$ correlated with a notable decrease in the friction force (panels b in Figure 1); from these observations we conclude that the critical velocity $v_c > 20 \text{ m/s}$. Accompanying the stick–slip motion are sharp variations in the number of confined molecules, as well as small dilations of the gap width. On the other hand, the approach of the steady sliding regime is signaled by a sharp drop in n_c (see Figure 1d for $v_s = 20 \text{ m/s}$) with subsequent variations in the gap width and n_c being small and erratic. Similar simulations for an external load of 132 MPa (corresponding also to a four-layer film, but now in its optimally structured well-layered configuration) resulted also in stick–slip motion for $v_s = 1 \text{ m/s}$. However, for sliding with $v_s = 10 \text{ m/s}$ the confined film collapsed to a three-layer structure via expulsion of a layer worth of molecules during a brief interval following a slip stage in the stick–slip cycle (Figure 2). The transition to a three-layer film is seen to be accompanied by increased (static) friction. Such shear-induced transitions in film thickness have indeed been observed experimentally.^{5,9b}

The two stages in the stick–slip cycles and the transition between them are accompanied by structural changes in the film. Thus, while the film in the stick stages exhibits a dynamical

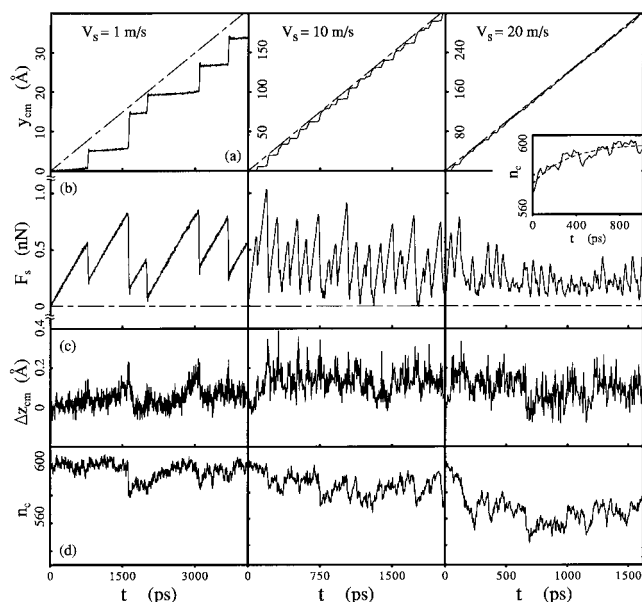


Figure 1. (a) Position of the center of mass of the spring-pulled upper solid block (y_{cm} , solid line), (b) sliding-spring force (F_s), (c) height variations of top block (Δz_{cm}), and (d) number of molecules in the confinement (n_c), plotted versus time (t), obtained from GCMC simulations of a four-layer junction under constant external load $P_{\text{ext}}^z = 73 \text{ MPa}$, sheared with spring velocities of $v_s = 1, 10$, and 20 m/s as indicated. The dashed line in (a) depicts $v_s t$. Note the stick–slip dynamics for $v_s = 1 \text{ m/s}$, decreasing for $v_s = 10 \text{ m/s}$ and further reduced for $v_s = 20 \text{ m/s}$ (approaching the steady-sliding regime). In the inset in the top panels for $v_s = 20 \text{ m/s}$ we display the time evolution of $n_c(t)$ following a sudden cut (denoted here as $t = 0$) of the sliding spring during the steady-sliding. This information was used to estimate the molecular flow relaxation time, τ_f (the dashed line indicates an exponential fit with $\tau_f = 300 \text{ ps}$). Distances, force, and time in units of \AA , nN, and ps, respectively.

phase characterized by a layered structure with high degree of intralayer order (both in the interfacial layers and inside the film), the transition to a slip stage is signaled by structural transformation of the interior layers in the film (which continues to maintain a rather distinct layered structure) into a dynamical phase with the intralayer order in these layers characterized by regions of a highly dislocated two-dimensional (2D) defective solid coexisting with 2D ordered (close-packed) islands (these islands appear to nucleate ordering of the layers¹⁸ when a subsequent stick stage develops). The latter dynamical phase appears to be distinct from the less ordered (“fluidized”^{10a}) phases that are found during the steady-sliding and superkinetic regimes. In this context we remark that in simulations employing a stiff pulling spring (i.e., $k_s \rightarrow \infty$) atomic-scale stick–slip processes were found (with a slip length corresponding to the in-layer intermolecular distance in the slip direction), but with no accompanying intralayer disordering; instead the stick–slip dynamics occurred here via a sequence of intralayer-registry-change transitions (intralayer shuffle), each involving collective motion of the (ordered) interior layers past one another.

The central issue that we would like to address now is whether the friction in such boundary lubricated systems can be controlled. For example, can a transition to the ultralow-friction superkinetic regime be induced by other means, without having to slide the system with high velocities, $v > v_c$ (i.e., larger than 20 m/s in our case)? To this aim, a novel method for accessing low friction states of the confined lubricant is suggested by the aforementioned observations,¹² obtained from simulations of equilibrium states of the system, pertaining to the nature of transitions between equilibrium layered states of the film that

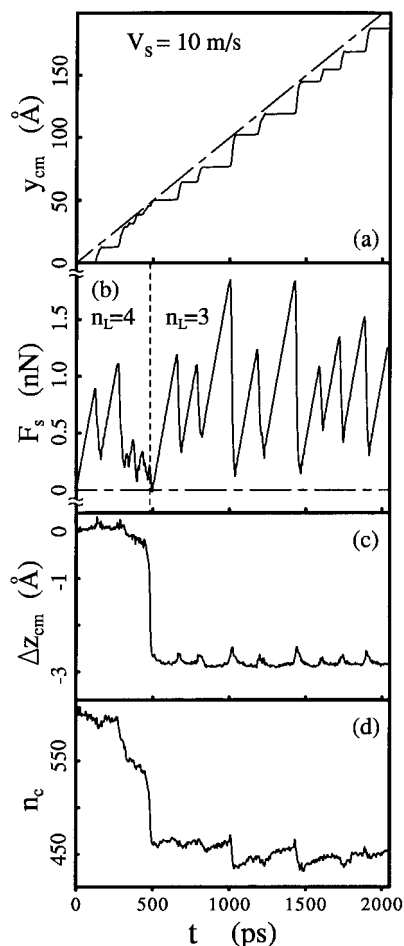


Figure 2. Same as Figure 1, but for a well-formed four-layer system sheared with $v_s = 10$ m/s under a constant load $P_{\text{ext}}^z = 132$ MPa. Note the sharp collapse of the confined film at $t \approx 500$ ps from $n_L = 4$ to $n_L = 3$, accompanied by a decrease in the gap width (c), expulsion of a layer-worth of confined molecules (d), and a pronounced increase in the static friction (peaks of the stick–slip cycles depicted by F_s in (b)).

are initiated by small (~ 1 Å) variation in the gap width. In this method dynamic controlled coupling is established between the molecular and flow degrees of freedom of the sheared lubricant and a mechanically driven mode. Here this method of friction control takes the form of applied directional small-amplitude oscillatory variations of the gap width.

Prior to exploring the effect of oscillations of the confining gap on sliding friction, we apply to the layer-ordered system periodic oscillations of the gap width and allow the system to evolve until a steady state is achieved;¹⁹ an illustration of the change in the degree of order in a four-layer confined film caused by such oscillations (with an amplitude of 1.5 Å) is shown in Figure 3. Results of sliding simulations are shown in Figure 4, confirming our expectations pertaining to the influence of directional oscillations of the confining boundaries on the sliding dynamics and friction in the lubricated junction. In particular, small-amplitude (1.5 Å) periodic variations (triangular drive with a velocity $v_{\text{osc}} = 15$ m/s) of the gap width for the four-layer film result (for a sliding velocity $v_s = 1$ m/s) in a most significant reduction of the frictional resistance and obliteration of the stick–slip dynamics, that is, transition to an ultralow friction state, i.e., the superkinetic regime (compare the left column in Figure 4a,b to the corresponding oscillation-free case shown for $v_s = 1$ m/s in Figure 1a,b). This transition is accompanied by a precipitous decrease in n_c and the normal

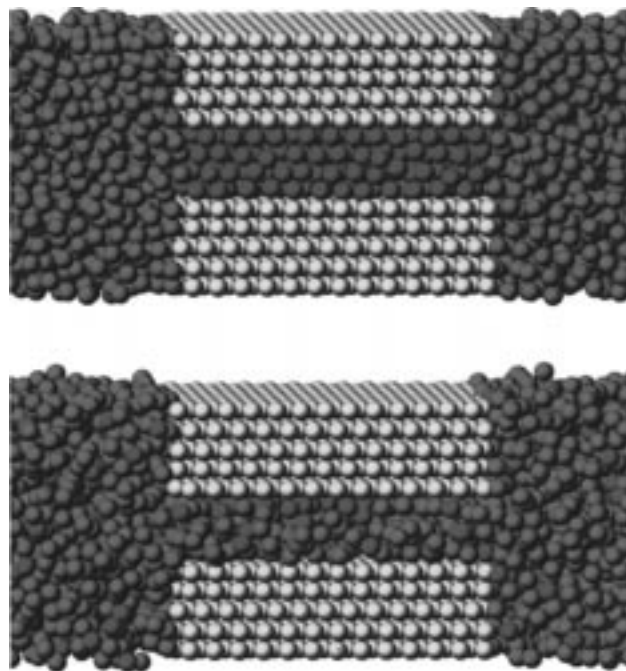


Figure 3. Atomic configurations obtained from grand canonical molecular dynamics simulations of a fluid lubricating the gap between opposing solid boundaries (yellow spheres). The upper equilibrium configuration was recorded for a gap width of 15.25 Å showing organized organization of the confined fluid molecules (in purple) into four ordered layers; the liquid molecules outside the confinement are depicted in green. The bottom figure, recorded during a small-amplitude (1.5 Å) oscillation of the gap width, illustrates disordering of the layered structure in the confinement accompanied by flow of molecules in and out of the confined region.

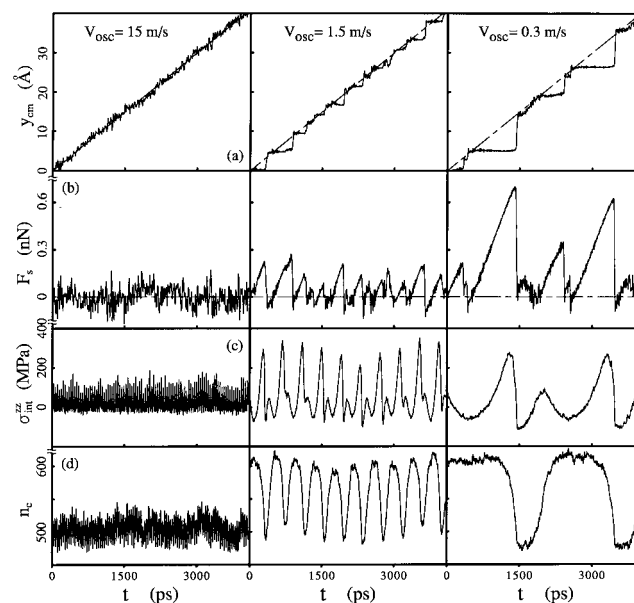


Figure 4. Same as Figure 1 with $v_s = 1$ m/s, but under directional oscillations of the top solid block along the z -axis (normal to the shear plane), using a triangular waveform with an amplitude of 1.5 Å and velocities $v_{\text{osc}} = 15, 1.5,$ and 0.3 m/s, as indicated. In panels (c) we display the time variations of the normal component of the internal stress on the confining boundaries, $\sigma_{\text{int}}^{\text{zz}}$ (in units of MPa). Note the transition to a superkinetic regime for the highest oscillation velocity and the intermittent well-defined stick–slip and superkinetic dynamics for the lowest one.

component of the internal stress on the boundaries, $\sigma_{\text{int}}^{\text{zz}}$. Since the transition to the superkinetic regime occurred under the influence of the out-of-plane oscillations already at a spring

sliding velocity $v_s = 1$ m/s, while for the oscillation-free case such transition requires velocities larger than 20 m/s, the effect of the oscillations may be interpreted as effectively lowering the critical velocity v_c in a most significant way. On the other hand, under directional oscillations at a lower frequency ($v_{\text{osc}} = 1.5$ m/s) a somewhat frustrated form of stick–slip dynamics is maintained (compare middle column in Figure 4a,b with the left column in Figure 1a,b), while oscillations at an even lower frequency ($v_{\text{osc}} = 0.3$ m/s) result in intermittent stick–slip (characterized by pronounced high static friction peaks, Figure 4b) and short periods of close to superkinetic sliding, accompanied by large variations in n_c and σ_{int}^z (with low values during the superkinetic intervals).

To understand and optimize the frequency dependence of the applied mechanical directional oscillatory coupling to the molecular shear flow motion, we suggest that the dominant operative relaxation time is that pertaining to molecular flow in-and-out of the confined zone, denoted by τ_f ; other relaxation processes, such as layering of the film, intralayer ordering, and the time for restoration of stick–slip dynamics after interruption of the directional oscillatory variation of the gap width while in the superkinetic state, are related to τ_f . To estimate τ_f we have cut the pulling spring during sliding in the superkinetic regime under constant load (see $v_s = 20$ m/s in Figure 1) and recorded the time evolutions of $n_c(t)$ (see inset in Figure 1). Fitting the increase in the number of confined molecules by an exponential form yields $\tau_f^{n_c=4} \sim 300$ ps. We now may estimate the Deborah numbers $D_e = \tau_f/\tau_{\text{osc}}$ (where τ_f and τ_{osc} are taken as the operative relaxation and drive times, respectively) with $\tau_{\text{osc}} = 6 \times 10^{-10}$ m/ v_{osc} , yielding for $v_{\text{osc}} = 15$ m/s (i.e., $\tau_{\text{osc}} = 40$ ps), $D_e = 7.5$; that is, in this regime the system is driven out of dynamic equilibrium conditions, resulting in reduced frictional resistance (superkinetic regime), as observed in the simulations (Figure 4a,b for $v_{\text{osc}} = 15$ m/s). On the other hand, for $v_{\text{osc}} = 1.5$ m/s (i.e., $\tau_{\text{osc}} = 400$ ps), $D_e = 0.75$ and a somewhat “mixed” stick–slip dynamics occurs reflecting the ability of the confined molecular system to only partially relax and explore its intrinsic dynamical states at any value of the externally applied gap variations, while for $v_{\text{osc}} = 0.3$ m/s (i.e., $\tau_{\text{osc}} = 2000$ ps), $D_e = 0.15$ resulting in intermittent well-defined stick–slip and steady-sliding intervals.²⁰ In fact, in the latter two cases other molecular relaxations and drive characteristic times (such as the one associated with the sliding spring-driven motion) may become operative, and they, together with τ_f , should be considered in estimating the effective D_e .

It is of some interest to model the above findings obtained via atomistic simulations by a generalization of a phenomenological rate and state (RS) approach²¹ for boundary lubrication proposed recently²² by Carlson and Batista (CB). In this model the friction force $F_0(\dot{y}_{\text{cm}}, \theta(t))$ is taken to depend on the center of mass velocity, \dot{y}_{cm} , of the block (of mass M) pulled by the spring, and on a state variable $\theta(t)$, representing the state of the lubricant. The state variable (order parameter) is constrained to vary dynamically between a maximum value θ_{max} (ordered state) and a minimum value θ_{min} (disordered state), satisfying the equation

$$\dot{\theta} = \frac{(\theta - m(t)\theta_{\text{min}})(m(t)\theta_{\text{max}} - \theta)}{\tau} - \alpha(\theta - m(t)\theta_{\text{min}})\dot{y}_{\text{cm}} \quad (1)$$

with the ordering rate proportional to τ^{-1} and $1/\alpha$ playing the role of a characteristic disordering distance.²² In the original CB model, and for the oscillation-free case, $m(t) \equiv 1$.

As discussed above,¹² we have found from the simulations that small-amplitude variations of the width of the confining

gap from a well-formed layered state cause significant changes in the structural, dynamic, and rheological properties of the lubricant. To model such effects, caused by an applied oscillatory variation with a frequency $\omega_{\text{osc}} = 2\pi/\tau_{\text{osc}}$, rate and state models can be generalized by relating some of the model parameters, specifying the state and/or properties of the lubricant, to external control variables. We present here one simple example of such a generalization, where we use a modulation function (i.e., $m(t)$ in eq 1) to represent direct external control of the state of the lubricant; here we take $m(t) = 1 - A_m \sin^2(\omega_{\text{osc}}t/2)$. The time-dependent modulation (control) of the extremal values (θ_{max} and θ_{min}) of the order parameter models here states of the lubricant, accessed via an external oscillatory drive, which are characterized by maximal and minimal values of the order parameter that are smaller than in the absence of such imposed oscillations.

To complete the model the equation of motion for the spring-pulled block and the expression for the friction force F_0 are taken after CB (see eqs 1 and 2 in ref 22). It is convenient now to rescale variables $\theta' = (\theta - \theta_{\text{min}})/(\theta_{\text{max}} - \theta_{\text{min}})$, and $\theta_0 = \theta_{\text{min}}/\Delta\theta$, $\theta_1 = \theta_{\text{max}}/\Delta\theta$, and $\tau' = \tau/\Delta\theta$, where $\Delta\theta = \theta_{\text{max}} - \theta_{\text{min}}$, as well as denote $n(t) = 1 - m(t) = A_m \sin^2(\omega_{\text{osc}}t/2)$. With this rescaling (dropping the primes) and notations the equations of the generalized rate and state (GRS) model are

$$M\ddot{y}_{\text{cm}} = -k_s(y_{\text{cm}} - v_s t) - F_0 \quad (2)$$

$$F_0 = \theta_{\text{min}} + (\theta_{\text{max}} - \theta_{\text{min}})\theta + \beta\dot{y}_{\text{cm}} \quad (3)$$

$$\dot{\theta} = (\theta + \theta_0 n(t))(1 - \theta - \theta_1 n(t))/\tau - \alpha(\theta + \theta_0 n(t))\dot{y}_{\text{cm}} \quad (4)$$

Note that when $n(t) \equiv 0$ the oscillation-free CB model is recovered. The first term in eq 2 is the (experimentally measured) spring force, F_s , and from eq 3 it is seen that in a more ordered state (larger value of the dynamical state variable θ , e.g., $\theta \sim 1$) the friction force is larger than in a disordered state (e.g., $\theta \sim 0$).

To compare the results of the model to our simulations, we use $k_s = 0.8$ nN (as in the simulations) and $M = 24\,450$ amu (the combined mass of the sliding block and half of the confined lubricant used in the simulations²³). For the extremal values of the order parameter we take $\theta_{\text{max}} = 0.8$ nN and $\theta_{\text{min}} = 0.19$ nN, guided by the variations of the spring force in the oscillation-free simulations at $v_s = 1$ m/s (see F_s in the left column in Figure 1b), and for the amplitude we take $A_m = 0.9$. The other parameters of the model ($\alpha = 0.5 \text{ \AA}^{-1}$, $\beta = 0.2$ nN·ps/Å, and $\tau = 7.55$ ps) were determined by attempting to reproduce the general behavior (frequency of stick–slip events and their amplitudes) for the oscillation-free cases (Figure 1b). The results of the model displayed in Figure 5 for oscillation-free sliding (i.e., $n(t) \equiv 0$ in eq 4) at $v_s = 1, 10$, and 20 m/s exhibit rather adequate correspondence with those predicted through the MD simulations (compare to Figure 1).

Most remarkable is the correspondence between results of the MD simulations (Figure 4) and the model results shown in Figure 6 for sliding with $v_s = 1$ m/s and for three oscillation periods ($\tau_{\text{osc}} = 40, 400$, and 2000 ps), which are the same as those used in the corresponding MD simulations. In the latter a saw-tooth drive was employed, while for convenience in displaying the model equations we used sinusoidal oscillations; we note here that very similar results are obtained by integrating eqs 2–4 with the modulating function taking the form of a saw-tooth pattern. While refinements and/or alternative ways of incorporating the effect of external drives in rate and state models are certainly possible (and are being explored by us),

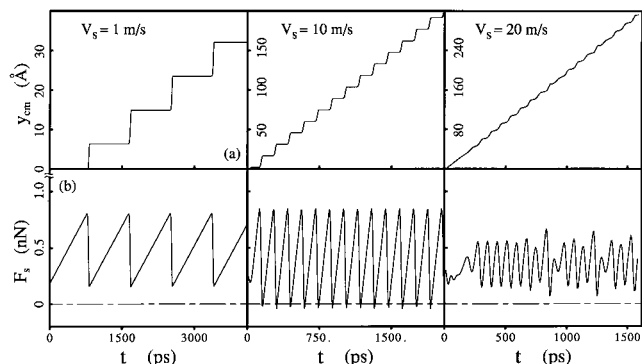


Figure 5. Results for oscillation-free sliding for three spring velocities ($v_s = 1, 10,$ and 20 m/s) obtained via the CB rate and state model, with the parameters given in the text. Note the close correspondence between these results and those predicted by the MD simulations given in Figure 1a,b.

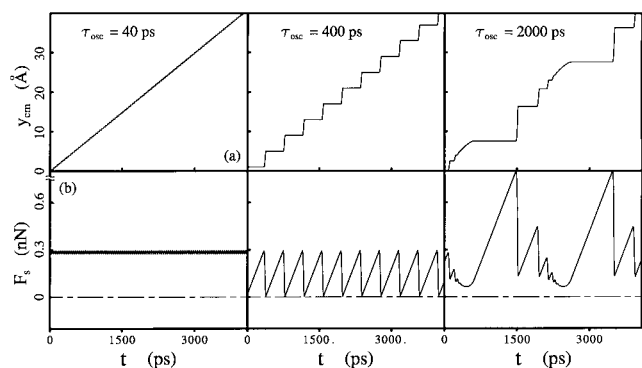


Figure 6. Results for sliding with oscillations for three oscillation periods ($\tau_{osc} = 40, 400,$ and 2000 ps) and $v_s = 1$ m/s, obtained via the generalized rate and state model; these oscillation periods are the same as those used in the simulations (see Figure 4). The parameters of the GRS model are the same as those used in Figure 5. Note the correspondence between these results and those predicted by the MD simulations (Figure 4a,b). In particular, note the steady sliding and the notable reduction in the friction (as measured by the spring force, F_s) caused by the oscillations at the highest oscillation frequency (compare $\tau_{osc} = 40$ ps with the corresponding oscillation-free case shown in the left column in Figure 5); we remark that in the MD simulations (Figure 4, left column) oscillations with $\tau_{osc} = 40$ ps resulted in ultralow friction (superkinetic regime).

our present approach, consisting of modulation of the extremal values of the order parameter, captures many of the essential features revealed by the MD simulations.

In summary, in this study we proposed and demonstrated through GCMD simulations a novel method for controlling the shear dynamics and friction in thin-film boundary lubrication, through directional coupling of small-amplitude (of the order of 1 \AA) oscillations of the solid boundary (normal to the shear plane) to the transverse shear flow of the film molecules. The directional oscillations frustrate ordering in the film, maintaining it in a nonequilibrium dynamic state, and their effect can be controlled through selection of the oscillation period τ_{osc} , with the control parameter being $D_e = \tau_f / \tau_{osc}$, where τ_f is a characteristic time for molecular relaxation flow in-and-out of the oscillating confined junction, though other characteristic structural relaxations may also be operative under other circumstances. Finally, a generalized rate and state model was introduced, yielding results in close correspondence with those

predicted by the atomistic simulations. Experimental observations pertaining to control of friction through directional coupling have been most recently made.^{24–26}

Acknowledgment. This work is supported by the AFOSR and the DOE. Simulations were performed at the Pittsburgh Supercomputing Center, the National Energy Research Scientific Supercomputing Center, Berkeley, CA, and the Georgia Tech Center for Computational Materials Science.

References and Notes

- (1) Bhushan, B.; Israelachvili, J. N.; Landman, U. *Nature* **1995**, *374*, 607.
- (2) Landman, U.; Luedtke, W. D.; Gao, J. *Langmuir* **1996**, *12*, 4514.
- (3) *Microtribology and its Applications*; Bhushan, B., Ed.; Kluwer: Dordrecht, 1997.
- (4) Israelachvili, J. N. *Intermolecular and Surface Forces*, 2nd ed.; Academic Press: New York, 1992.
- (5) Israelachvili, J. N.; McGuiggan, P. M.; Homola, A. M. *Science* **1988**, *240*, 189.
- (6) Van Alster, J.; Granick, S. *Phys. Rev. Lett.* **1988**, *61*, 2570.
- (7) Granick, S. *Science* **1991**, *253*, 1374.
- (8) Yoshizawa, H.; Israelachvili, J. *J. Phys. Chem.* **1993**, *97*, 11300.
- (9) (a) Klein, J.; Kumacheva, E. *Science* **1995**, *269*, 816; and *J. Chem. Phys.* **1998**, *108*, 6996. (b) Kumacheva, E.; Klein, J. *J. Chem. Phys.* **1998**, *108*, 7010.
- (10) (a) Thompson, P. A.; Robbins, M. O. *Science* **1990**, *250*, 792. (b) Thompson, P. A.; Robbins, M. O.; Grest, G. S. *Isr. J. Chem.* **1995**, *35*, 93.
- (11) Gao, J.; Luedtke, W. D.; Landman, U. *Science* **1995**, *270*, 605.
- (12) (a) Gao, J.; Luedtke, W. D.; Landman, U. *J. Phys. Chem. B* **1997**, *101*, 4013. (b) *Phys. Rev. Lett.* **1997**, *79*, 705.
- (13) Yoshizawa, H.; Chen, Y.-L.; Israelachvili, J. N. *Wear* **1993**, *168*, 161.
- (14) Reiner, M. *Phys. Today* **1964**, (January), 62.
- (15) Gohar, R. *Elastohydrodynamics*; Horwood: Chichester, 1988; p 204.
- (16) A commensurate solid–liquid system is simulated here since shearing at high velocities a liquid lubricant of spherical molecules with dimensions incommensurate with the underlying confining crystalline boundaries results in slip of the lubricant molecules at the solid boundaries.^{12b}
- (17) In these simulations the atoms of the solid boundaries were treated statically. Including dynamics of these atoms with interactions characteristic of metals did not influence our result in any discernible way.
- (18) Persson, B. N. J. *Phys. Rev. B* **1995**, *51*, 13568.
- (19) In simulations where both the gap oscillations and pulling of the spring were applied simultaneously from the start, the same results as those shown below (Figure 4) were obtained past a short transient interval.
- (20) Note that it is the ratio between the molecular relaxation time and the characteristic drive time which enter our considerations rather than the absolute values of these quantities. Consequently, for other lubricants (with more complex molecular structures), characterized by longer relaxation times (e.g., *n*-hexadecane), significantly lower drive frequencies are required to achieve the friction-control effect demonstrated here (J. Gao, W. D. Luedtke, U. Landman, unpublished results). Additionally, when the molecular flow characteristic time, τ_f , is the dominant operative relaxation time, as is the case here, simulations for larger confinements (that is, larger confining surfaces, associated with larger values of τ_f) also require lower drive frequencies. Similar considerations apply to the friction-spring force-constant and pulling velocities.
- (21) Ruina, A. L. *J. Geophys. Res.* **1983**, *88*, 10359. Rice, J. R.; Ruina, A. L. *J. Appl. Mech.* **1983**, *50*, 343.
- (22) Carlson, J. M.; Batista, H. F. *Phys. Rev. E* **1996**, *53*, 4153.
- (23) We used this effective value for M since we observed in the simulations that part of the lubricant adhered to the sliding block and the slip plane was inside the lubricant film. Taking for M just the mass of the block does not affect the results of the model in any significant manner.
- (24) Heuberger, M.; Drummond, C.; Israelachvili, J. N. *J. Phys. Chem. B* **1998**, *102*, 5038.
- (25) Dinelli, F.; Biswas, S. K.; Briggs, G. A.; Koslov, O. V. *Appl. Phys. Lett.* **1997**, *71*, 1.
- (26) The influence of macroscopic dynamic loads on frictional resistance in lubricated machine elements has been used empirically and phenomenologically modeled (Polycarpou, A. A.; Soom, A. *J. Tribol.* **1995**, *117*, 255), but molecular-scale effects have not been considered.